

Particle Swarm Optimization of Balanced Antipodal Vivaldi Antenna for Ultra Wide Band Imaging Applications

Abdul Aziz*, Abdul Sattar Malik†, Arslan Azhar*, Muhammad Abrar†, H. M. T. Mustafa**

* Islamia University of Bahawalpur, †Bahauddin Zakariya University Multan - Pakistan.

** Department of Electrical Engineering, University of the Punjab Lahore – Pakistan

ABSTRACT

The aim of this paper is to optimize a Balanced Antipodal Vivaldi Antenna (BAVA) to obtain a design compatible with the FCC UWB regulations (return loss less than -10dB for 3.1 to 10.6GHz) as well as having a high gain, low cross polarization, better group delay and smaller size as compared to several published designs. The paper also illustrates the important decisions taken in the design process to help reducing the optimization time and resources. The BAVA has been optimized to reduce antenna return loss and enhance directivity by directly applying Swarm Particle Optimization (PSO) algorithm on a full scale parametric simulation model of BAVA in FEKO suite. Finally, several important radiation characteristics are obtained and compared using EMSS FEKO and Ansoft HFSS to ensure consistency in results.

Index Terms— Antipodal Vivaldi antenna, particle swarm optimization, ultra-wide-band antenna, OPTFEKO, tumor detection.

I. INTRODUCTION

Ultra-Wide-Band (UWB) Antennas are the subject of extensive research in past few years due to their great potentials in extensive array of applications including tumor detection, See-Through-Wall (STW), Wall Imaging, and high data rate communication systems. The FCC has introduced Ultra-Wide-Band (UWB) standard [1] for specified microwave imaging applications such See-Through-Wall (STW), Ground Penetrating Radar (GPR) and Bio-medical imaging applications. Common frequencies for all such application are 3.1-10.6GHz and for those frequencies, the antenna should operate below -10dB (S11). High resolution, high data rate, small antenna dimensions and relatively less occupied bandwidth are some of the reasons that have made the UWB antennas a topic of growing interest for research in the recent years.

Pulse based radar imaging systems operate by transmitting short-time microwave pulses toward the object/s of interest. The pulse after having reflections from various objects is recorded by the same or another broadband receiver antenna depending upon the mode of operation of radar (Monostatic or Bistatic respectively). Such reflections are dependent on electrical properties of the objects i.e. dielectric constant. For example, the UWB application of breast tumor detection involves analysis of reflected microwave pulses to locate and differentiate tumor from healthy tissues [2] [3]. The resolution of the image recreated this way is inversely proportional to the bandwidth of the transmitting antenna hence a wide bandwidth antenna is preferred.

The Vivaldi antenna originally proposed by Gibson in 1979 [4], is a type of travelling wave antenna having a tapered exponential profile of radiating element which gives the antenna the extremely wide operating bandwidth. To avoid bandwidth limitations due to coupled feed in the original design, Gazit [5] proposed a modified version of this antenna called Antipodal Vivaldi in which the antenna was fed directly

by coaxial cable. Finally, stacking an additional ground layer on top of the antenna was suggested in [6] to significantly reduce the cross-polarization and improve UWB pulse transmission. This antenna is referred to as Balanced Antipodal Vivaldi Antenna (BAVA) and is the antenna of choice for this work. The high directivity, low cross-polarization and good matching characteristics of BAVA aids in rejection of unwanted reflections from surroundings such as in case of See-Through-Wall applications. Such features make BAVA an ideal candidate for pulse-radar based microwave imaging applications.

Unlike narrowband antennas, designing UWB antennas for radar based imaging application is challenging because a UWB antenna must exhibit acceptable and near-uniform radiation characteristics such as S11, gain, cross-polarization etc for large bandwidths. The objective of this work is to optimize a BAVA to have $S_{11} < -10\text{dB}$, moderate to high gain, small group delay and a compact size.

Number of UWB antennas have been proposed recently ([7], [8], and [9]) but a majority of these designs do not satisfy S11, Gain, group delay and physical size requirements of microwave imaging applications *in a single design*. For example, UWB antenna presented in [7] though having small size, is lacking both reasonable gain and low S11.

Bourqui and Okoniewski [10] have optimized BAVA for operation in canola oil ($\epsilon_r = 2.5$), a requirement for antennas operating in Tissue Sensing Adaptive Radar (TSAR) systems, but since the mismatch at substrate-canola oil can be made negligible by selecting appropriate substrate, so reducing S11 is not as challenging in this situation as in the case of BAVA operating in air. This is true because the minimum dielectric constant of most readily available substrate sheets is 2.2 which create a mismatch with surrounding air resulting in increased S11.

In this work, first a fully parametric model of Balanced Antipodal Vivaldi Antenna is created in FEKO. This model is optimized using built-in Particle Swarm Optimization (PSO) algorithm which varies physical parameters of antenna such as aperture opening rate to reduce S11 and increase endfire radiation throughout UWB. The antenna is then simulated in FEKO ver 5.5 to determine radiation characteristics of antenna and simulated again in HFSS to validate the results.

II. ANTENNA GEOMETRY

An exploded view of the construction of antenna is shown in Fig. 1. The antenna consists of three copper layers and four substrate layers. (1.524mm, Neltec NY9220, $\epsilon_r=2.2$). Two external copper layers are connected to the ground of feed while the central conductor is connected to the inner conductor of the feed. The copper layers are supported by two inner substrate layers and are then sandwiched between two external substrate layers. The feed structure is a gradual transition from Stripline to Tri strip line, see Fig. 2. In the stripline, the central conductor width increases linearly while ground layers width decreases exponentially to maintain constant input impedance of 50 Ohms.

The plane of antenna is constructed in $y=0$ plane with aperture opening along the x-axis.

A. Antenna Parameters and Curve Equations.

In Fig. 2, L and $W+W_d$ are overall dimensions of antenna. W_g , W_s and W_a are widths of ground layers, central conductor and antenna aperture respectively at locations specified in Fig. 2. L_t and L_a are lengths corresponding to transition and antenna aperture.

E_t , E_f and E_a are exponential curves given by the following relation:

$$z = \pm A e^{P(x-B)} + C \quad (1)$$

definition of A (*scaling factor*), P (*the exponential rate*), B (*the shifting value*) and C (*the offset*) for three curves (E_t , E_f and E_a) is given in TABLE I.

B. Parametric Study of Antenna

To minimize the dielectric constant mismatch between substrate layers and surrounding air, a low dielectric constant substrate is preferable. However, the high value of dielectric constant improves endfire radiation, thus the overall directivity. Hence, we chose Neltec NY9220 (1.524mm) which has a reasonable compromise at $\epsilon_r=2.2$.

One of the aims of this work is to reduce overall dimensions of the antenna below frequent threshold of 10cm by 10cm for BAVA operating in UWB. Increasing the aperture width or overall width reduces S11 and improves endfire radiation. However, a large width is not only unpractical but may also contribute to pulse deterioration. Exponential rate of the curve 'Ea' should not be too large as well.

A sharp increase in curve Ef enhances end fire radiation but degrades S11. In fact, one of the techniques used in this work is to enhance end fire radiation by allowing sharp Ef instead of increasing the overall antenna width, the resulting augmented S11 was then reduced by optimizing other antenna parameters such as Wa, Wts and Pa.

III. OPTIMIZATION OF ANTENNA GEOMETRY

A. Particle Swarm Optimization (PSO)

The selection of appropriate algorithm for optimization of the antenna is a complex procedure and depends on various factors such as number and range of parameters. Feko 5.5 offers two major types of optimization algorithms other than PSO, namely Genetic Algorithm (GA) and Simplex (Nelder-Mead). The Simplex is a hill climbing method and is strongly dependent on specific starting parameters values, a fact that renders this algorithm inappropriate for optimizing UWB antennas. Whereas the PSO has been observed to do better than GA in terms of computational time and resources.

Originally introduced by Kennedy and Eberhart in 1995 [11], the Particle Swarm Optimization is stochastic evolutionary computation technique originally developed to simulate the movement and intelligence of swarms. As an optimization method, PSO is especially suited for global search of solution parameters i.e. the optimization process is independent of initial parameters.

In PSO algorithm, a "particle" is defined by its position (a possible solution) in D-dimensional search space and velocity (rate of change of position). The particle adjusts its velocity iteratively by comparing the current position with the best position of particle in past (pbest, individual best) and also with the best position of most optimistic particle in swarm (gbest, global best) using a fitness function which measures closeness of current value with optimum value. Each particle is initialized with random position before iteratively generating position and velocity vectors after each time step.

If for i^{th} particle, "k" is the number of iteration and "d" is the quantity in D-dimensional search space, then the velocity (v) and position (x) of i^{th} particle is evaluated using following equalities:

$$v_{id}^{k+1} = v_{id}^k + c_1 r_1^k (pbest_{id}^k - x_{id}^k) + c_2 r_2^k (gbest_{id}^k - x_{id}^k) \quad (2)$$

$$x_{id}^{k+1} = x_{id}^k + v_{id}^{k+1} \quad (3)$$

Where v_{id}^k is velocity and x_{id}^k is position at its k time. $pbest_{id}^k$ is the most optimum "d" dimension quantity of individual "i" particle at "k" time. In contrast, $gbest_{id}^k$ is the best global dimension quantity in whole swarm for "i" particle at k time. The second term in Eq. 2 is the cognition part and represents the personal experience of particle while the third term is the measure of co-operation between the particles and thus is called social component. Acceleration constants c_1 and c_2 are defined by user to regulate the changing speed of the particle and r_1 and r_2 are random numbers. A particle may follow the optimist value in its

surrounding instead of the whole swarm; this is known as local PSO and contains multiple smaller neighborhoods as compared to one large neighborhood in global PSO. The local PSO is essential in (a) avoiding premature convergence and (b) efficient exploration of the whole search space.

Although slight modifications have to be made to the original PSO for solving multi-goal optimization problems (including the antenna problem in this paper) but the underlying basic principles are the same as explained above.

The BAVA geometry is optimized to achieve two goals: to reduce S11 throughout UWB and to maximize end fire radiation. Since the PSO works more efficiently with reduced number of search parameters, hence transition parameters (W_t , W_s , W_g ...) and aperture parameters (W_a , L_a ...) are optimized independently and each successful optimization of one set was followed by optimization of another set until desired goals are achieved. This method was found to be converging faster as compared to a single run in which all parameters were optimized at once.

B. Reduction in Solution Time

A typical BAVA geometry took about 45 minutes to be solved for UWB using FEKO (method of moments) on a core i3 2.1GHz processor. A successful optimization required at least 70 of such cycles which means total time taken by optimization is at least $45 \times 70 \approx 50$ h.

It was observed that most of the computational time was consumed in solving the problem at the boundaries formed by substrate and adjoining copper layers /air. (This holds because FEKO uses method of moments (MOM) and surface equivalence principle (SEP) for solving multiple material problems). For optimization purpose only, we approximated this problem as a substrate-less BAVA (conductors only) submerged in free space having properties similar to substrate. ($\epsilon_r=2.2$). This decreased the solution time to approximately 12min per cycle as compared to original 45min. The resulting optimum design was simulated again in presence of substrate and surrounding air medium to obtain radiation-characteristics.

C. Optimum Antenna Parameters

The final values of antenna parameters after optimization are (in mm): $W_g=25.3$, $W_s=2$, $W_t=2.8$, $W_a=25.7$, $L=80$ $W=53.6$, $L_a=46.8$, $L_t=22.9$, and $W_d=2$.

IV. SIMULATION AND RESULTS

Antenna radiation characteristics were obtained by simulating antenna in FEKO v5.5 and Ansoft HFSS v13. The core solution process in FEKO is Method of Moments (MOM) and we have utilized Finite Element Method (FEM) while solving the antenna problem in HFSS. MOM is a full wave solution of Maxwell's integral equations in *frequency domain* in which the electric and magnetic currents on antenna geometry are calculated to determine the solution. Whereas in FEM, whole antenna as well as surrounding finite volume of space is discretized into small tetrahedral spatial elements and solution is obtained by calculating the electric fields in such volumetric elements.

A. Field Patterns

As stated previously, a directive antenna is preferable for near field imaging as well as for the detection of object from electrically large distance such as in case of See-Through-Wall applications. In fact, one of the two goals of the optimization in this work has been the improvement of end fire radiation throughout FCC's UWB bandwidth. Fig. 3 shows a three dimensional far field gain pattern at 3, 5, 7, and 10GHz in decibels. A polar plot of gain in $y=0$ plane for the same specifications is given in Fig. 4. The antenna gain varies between 8 and 9dB for UWB frequencies above 5GHz (see Fig. 5). Note that gain/directivity of antenna rises with frequency because of increase in effective electrical size of antenna with increasing

frequency. Side lobes tend to increase with frequency as well but relatively large major lobe has been observed throughout the frequencies ranging from 3.1-10.6GHz.

Horizontal and vertical components of normalized electric far field in $y = 0$ plane for 3, 7 and 10GHz is given by Fig. 6. Note that the vertical component of electric far field in endfire direction is 70, 60 and 80dB more than corresponding horizontal unwanted components at 10, 7 and 3GHz respectively. Good cross-polarization characteristic are essential in limiting interference to antenna and improves quality of imaging system.

B. S-parameter

The FCC standardized the UWB antennas as those antennas having S11 below -10dB from 3.1 to 10.6GHz operating bandwidth. Since the antenna is electrically large at lower frequencies, so reducing S11 is especially challenging in lower half of the UWB (3.1-10.6GHz). S11 of antenna calculated by FEKO (MOM) and HFSS (FEM) is given in Fig. 7 and it can be observed that $S_{11} < -10\text{dB}$ as predicted by both simulation soft wares. Also note the significant similarity in resonance frequencies as calculated by FEKO and HFSS.

The Fig. 8 compare real, imaginary values and magnitude of input impedance of antenna. Negligible imaginary impedance and an impedance value of 50 ohm is essential for matching the antenna with coaxial cable.

C. Group Delay

Finally quantity of interest is *group delay*. A group delay is a measure of transit time of a signal through antenna versus frequency. It is defined as “the derivative of radian phase with respect to radian frequency”, mathematically:

$$GD = \frac{d\phi}{d\omega} \quad (4)$$

Where ϕ is angular phase (radian) and ω is angular frequency in rad/sec. “d” indicates derivative. Fig. 9 represent the group delay of antenna as simulated in HFSS. The overall group delay fluctuates 0 to 2 ns. Variations in group delay are one of the major causes of distortion in transmitted pulse.

V. CONCLUSION

A simple UWB antenna design procedure has been devised in which a full scale parametric geometry of Balanced Antipodal Vivaldi Antenna (BAVA) has been optimized successfully using Particle Swarm Optimization in FEKO to simultaneously have better matching, directivity/gain, group delay characteristics as well as having dimensions less than 10 by 10cm . The same optimization model can be extended easily to include variety of operating conditions for BAVA antenna which are specific to a number of microwave imaging applications or if more compactness is desired. Further work is underway to improve transient characteristics of the BAVA and to further optimize the antenna for FCC specified UWB applications.

REFERENCES

- [1] Federal Communications Commission, "Revision of part 15 of the commission's rules regarding ultra-wideband transmission systems, Memorandum Opinion and Order and Further Notice of Proposed Rule making, ET Docket 98-153, FCC 03-33," March 2003.
- [2] Semenov, S.Y.; Bulyshev, A.E.; Abubakar, A.; Posukh, V.G.; Sizov, Y.E.; Souvorov, A.E.; van den Berg, P.M.; Williams, T.C.; , "Microwave-tomographic imaging of the high dielectric-contrast objects using different image-reconstruction approaches," *Microwave Theory and Techniques, IEEE Transactions on* , vol.53, no.7, pp. 2284-2294, July 2005
- [3] Semenov, S. Y. et al., "Microwave tomography: Two-dimensional system for biological imaging," *IEEE Transactions on Biomedical Engineering*, Vol. 43, 869-877, 1996.

- [4] P. Gibson, "The Vivaldi aerial," in *Proc. 9th European Microwave Conference* pg 103-105, 1979.
- [5] Gazit, "Improved design of a Vivaldi antenna," *IEEE Proc. H*, pp. 89-92, 1988.
- [6] P. S. H. a. P. N. J. D. S. Langley, "Novel ultrawide-bandwidth Vivaldi antenna with low crosspolarisation," *Electron. Letters*, vol. 29, no. 23, pp. 2004-2005, 1993.
- [7] Jolani, F.; Dadashzadeh, G., "Design and optimization of compact balanced antipodal vivaldi antenna," *Progress In Electromagnetics Research C*, vol. 9, pp. 183-192, 2009.
- [8] S. A. Hosseini; Z. Atlasbaf; K. Forooraghi;, "Two new loaded compact planar ultra-wideband antennas using defected ground structures," *Progress In Electromagnetics Research*, vol. II, p. 165–176, 2008.
- [9] Ultra-Wideband (UWB) Antennas for Mobile Applications," in *Ultra-Wideband, 2007. ICUWB 2007. IEEE International Conference on* , Singapore, Sept. 2007.
- [10] J. Bourqui, M. Okoniewski and E. C. Fear, "Balanced Antipodal Vivaldi Antenna With Dielectric Director for Near-Field Microwave Imaging," *IEEE Transactions On Antennas And Propagation*, vol. 58, no. 7, pp. 2318-2326, 2010
- [11] Kennedy, J.; Eberhart, R.; , "Particle swarm optimization," *Neural Networks, 1995. Proceedings., IEEE International Conference on* , vol.4, no., pp.1942-1948 vol.4, Nov/Dec 1995

Curve	A	P	B	C
Et	$\frac{W_{ts} - W_g}{2 * (e^{P_t * L_t} - 1)}$	P_t	0	$\frac{W_g}{2} - A_t$
Ef	A_f	P_f	L_t	$\frac{W_{ts}}{2} - A_f$
Ea	$\frac{W_{ts} + W_a}{2 * (e^{P_a * L_a} - 1)}$	P_a	L_t	$-\frac{W_{ts}}{2} - A_a$

TABLE I: EXPONENTIAL CURVE PARAMETERS

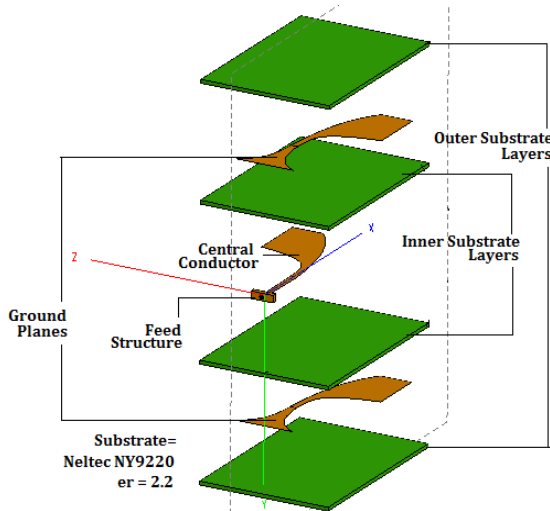


Fig. 1. Structure of Balanced-Antipodal-Vivaldi-Antenna

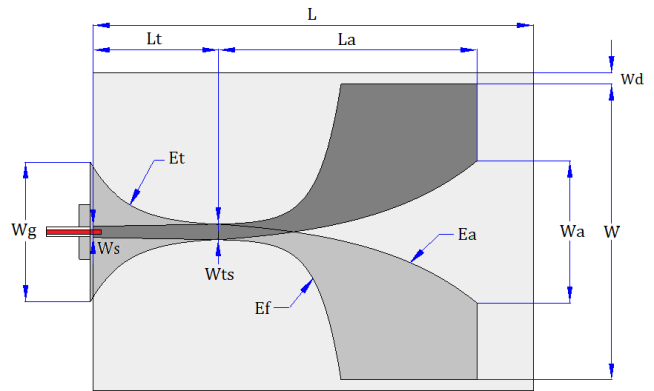


Fig. 2. Antenna Geometry and Parameters

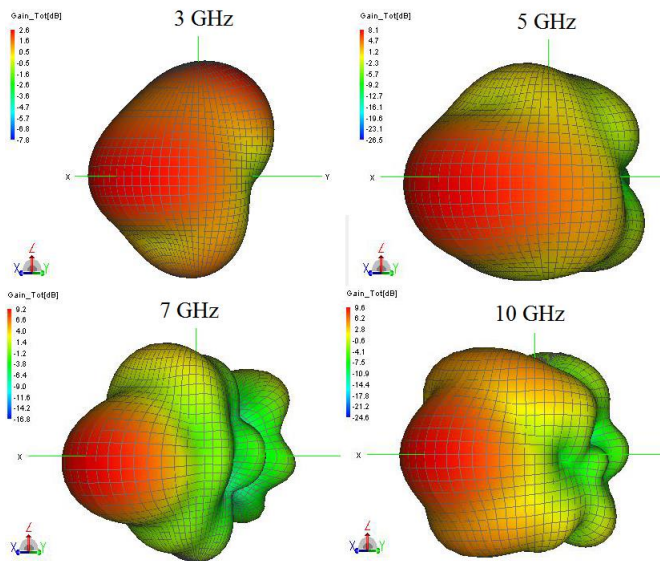


Fig. 3. Total Gain (dB) of antenna at four different frequencies in UWB. The gain plot is being viewed at $\theta = 90^\circ, \phi = 45^\circ$

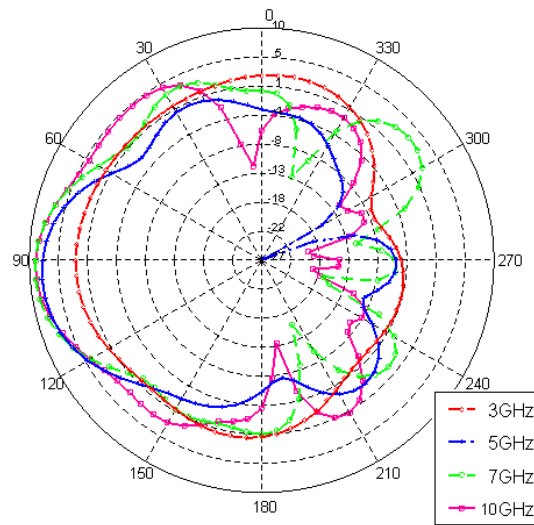


Fig. 4. Gain (db) $\theta = -180^\circ \rightarrow 180, \phi = 0^\circ$

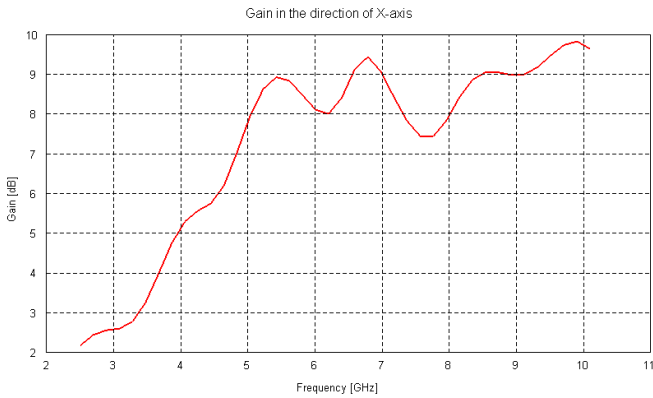


Fig. 5. Variation of Gain (dB) in principle direction with frequency.

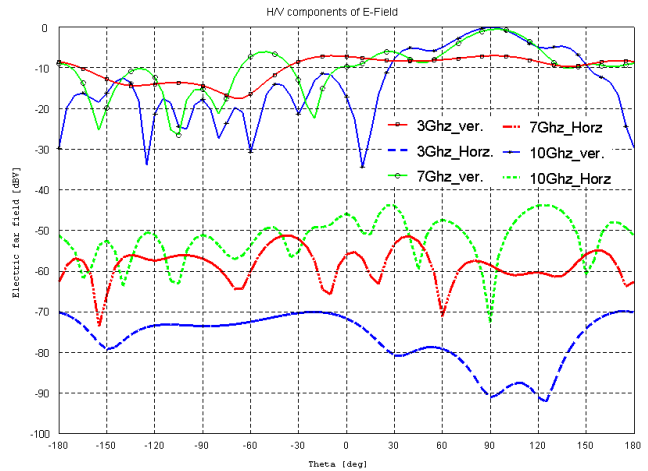


Fig. 6. Normalized horizontal and vertical components of E-far-Field ($\theta = -180^\circ \rightarrow 180, \phi = 0^\circ$) at 3,7 and 10GHz

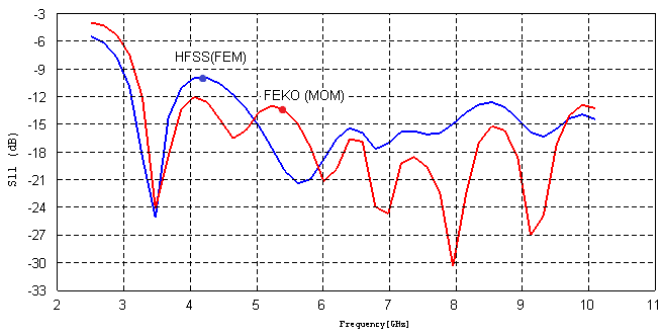


Fig. 7. Frequency variation of S11 at input port of antenna.

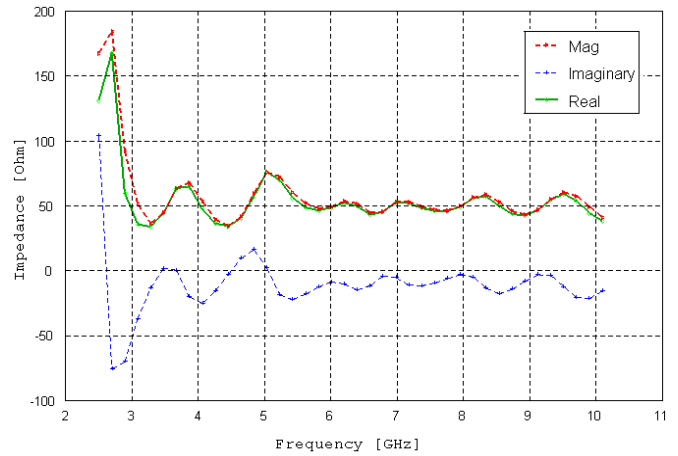


Fig. 8. Input Impedance of Antenna

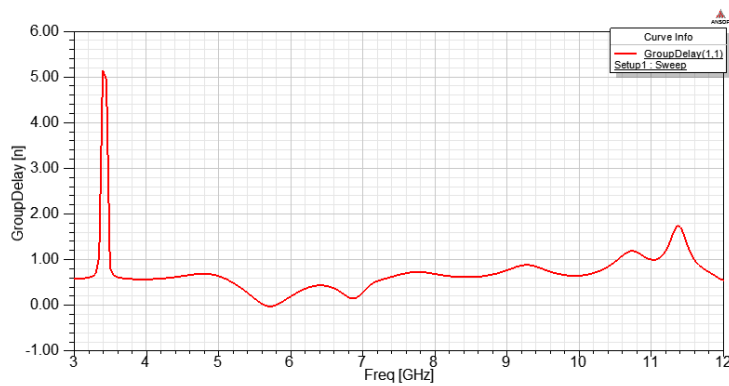


Fig. 9. Group delay (ns) versus frequency